Max-Planck-Institut
für Mathematik
in den Naturwissenschaften
Leipzig

Liquid bridges, edge blobs, and Scherk-type capillary surfaces

by

Paul Concus, Robert Finn and John McCuan

Preprint no.: 69 1999

Liquid Bridges, Edge Blobs, and Scherk-type Capillary Surfaces

Paul Concus, Robert Finn, and John McCuan

December 7, 1999

Abstract

It is shown that, with the exception of very particular cases, any tubular liquid bridge configuration joining parallel plates in the absence of gravity must change discontinuously with tilting of the plates, thereby proving a conjecture of Concus and Finn [*Phys. Fluids* **10** (1998) 39–43]. Thus the stability criteria that have appeared previously in the literature, which take no account of such tilting, are to some extent misleading. Conceivable configurations of the liquid mass following a plate tilting are characterized, and conditions are presented under which stable drops in wedges, with disk-type or tubular free bounding surfaces, can be expected. As a corollary of the study, a new existence theorem for H-graphs over a square with discontinuous data is obtained. The resulting surfaces can be interpreted as generalizations of the Scherk minimal surface in two senses: (a) the requirement of zero mean curvature is weakened to constant mean curvature, and (b) the boundary data of the Scherk surface, which alternate between the constants $+\infty$ and $-\infty$ on adjacent sides of a square, are replaced by capillary data alternating between two constant values, restricted by a geometrical criterion.

Key words: capillary surface, stability, contact angle, liquid bridge, mean curvature.

AMS subject classifications: Primary 76B45, 76D45, 53A10.
Secondary 49Q05, 53C42, 76E10.

Abbreviated title: LIQUID BRIDGES AND EDGE BLOBS

1 Introduction

There is a considerable literature on stability of liquid drops that form bridges between parallel plates in the absence of gravity. Earlier literature focused on drops whose bounding surfaces were constrained to pass through prescribed circular rings on the plates; more

recently papers have appeared concerning drops whose positions on the plates are not prescribed but whose configurations are determined by the natural boundary conditions of prescribed *contact angles* γ_1, γ_2 with the respective plates, arising from the underlying variational problem of minimizing mechanical (free surface plus wetting) energy. We mention the papers [1, 4, 14, 22, 32, 33], [35]–[38], [43]–[45] of which the sharpest (and in some ways definitive) results appear in [44]. In all cases, the drop surface is known to be rotationally symmetric and to have a constant mean curvature.

A consequence of the results in these references is that for any γ_1 and γ_2 in $[0, \pi]$ and sufficiently large V, there is a stable drop of volume V forming a tubular bridge that meets the plates in angles γ_1, γ_2; this bridge is determined uniquely up to rigid translation parallel to the plates [44].

In all of the literature just mentioned, the stability criteria are determined relative to perturbations of the fluid surfaces, for fixed and rigid plates. The effect of plate tilt on stability is first addressed in [24]; a more extensive discussion appears in [9]. Our intention in the present work is to show that if the plates are allowed to tilt, even infinitesimally, then with the exception of very particular cases, the fluid behavior as predicted by the idealized equations will differ dramatically from what is envisaged in current literature. The exceptional cases are exactly those for which the configuration is spherical, so that the tube appears as a spherical belt. We shall show that in all other cases, the dependence of the configuration on plate tilting is necessarily discontinuous. Since among all bridge configurations for given γ_1, γ_2, joining given parallel plates with varying volume, there is exactly one value $V = V_s$ that yields a spherical bridge, we will find that the cases of stability relative to plate tilting are indeed rare.

2 Discontinuous dependence

By a *tubular liquid bridge joining planes* Π_1, Π_2, we will understand an embedded surface $\mathcal{S}$ that is topologically a portion of a cylinder, bounded by two simple closed curves (*contact lines*) Σ_1 and Σ_2 that lie on the respective planes. We assume the closure of $\mathcal{S}$ to be of class C^1, and we suppose that $\Sigma_1 \cap \Pi_2 = \Sigma_2 \cap \Pi_1 = \emptyset$. We note that these definitions do not preclude surfaces that cross through the planes, although such surfaces would not be physically possible.

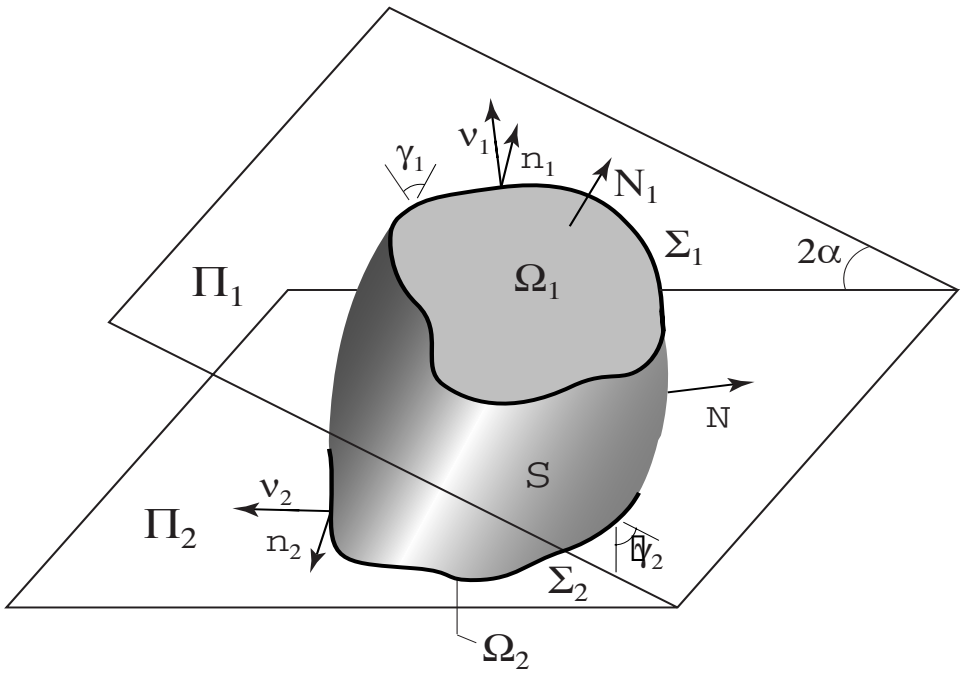

Figure 1: Tubular liquid bridge

We consider such a surface $\mathcal{S}$ having constant mean curvature H in a configuration for which Π_1 and Π_2 intersect in an angle 2α, $0 < 2\alpha < \pi$, as indicated in Figure 1. We suppose additionally that $\mathcal{S}$ meets Π_1, Π_2 in the respective constant contact angles γ_1, γ_2 measured interior to the tube enclosed by $\mathcal{S}$ and that $0 \leq \gamma_1, \gamma_2 \leq \pi$. We denote by Ω_1, Ω_2 the portions of the planes Π_1, Π_2 enclosed by Σ_1, Σ_2, respectively.

In the absence of an exterior gravity field, the position vector $\mathbf{x}$ on $\mathcal{S}$ satisfies

$$\Delta \mathbf{x} = 2H\mathbf{N} \tag{1}$$

where Δ denotes the invariant Laplacian on $\mathcal{S}$, and $\mathbf{N}$ is the unit exterior normal to $\mathcal{S}$. This normalization determines the sign of H, as positive if the curvature vector is directed exterior to the bridge, otherwise non-positive. Integrating $\Delta\mathbf{x}$ over $\mathcal{S}$ we obtain

$$2H \int_{\mathcal{S}} \mathbf{N} d\omega = \oint_{\Sigma} \frac{\partial \mathbf{x}}{\partial n}\, ds = \oint_{\Sigma} \mathbf{n}\, ds \tag{2}$$

where $\Sigma = \Sigma_1 \cup \Sigma_2$, and $\mathbf{n}$ is the unit conormal to $\mathcal{S}$ on Σ. We find for each plane Π_j, $j = 1, 2$,

$$\mathbf{n}_j = (\mathbf{n}_j \cdot \mathbf{N}_j)\mathbf{N}_j + (\mathbf{n}_j \cdot \nu_j)\nu_j = \mathbf{N}_j \sin\gamma_j + \nu_j \cos\gamma_j \tag{3}$$

where $\mathbf{N}_j$ is the unit normal to Ω_j exterior to the volume enclosed by $\mathcal{S}$, Ω_1, and Ω_2, ν_j is the exterior unit normal to Σ_j in Π_j, and $\mathbf{n}_j$ is the unit conormal to $\mathcal{S}$ on Σ_j (see Figure 1). We have

$$\oint_{\Sigma_j} \nu_j\, ds = \int_{\Omega_j} \nabla(1) d\omega = 0. \tag{4}$$

Also, denoting the bridge interior by $\mathcal{I}$, we have

$$\begin{aligned} \int_{\mathcal{S}} \mathbf{N} d\omega &= \int_{\mathcal{S}\cup\Omega_1\cup\Omega_2} \mathbf{N} d\omega - |\Omega_1|\mathbf{N}_1 - |\Omega_2|\mathbf{N}_2 \\ &= \int_{\mathcal{I}} \nabla(1) d\mathbf{V} - |\Omega_1|\mathbf{N}_1 - |\Omega_2|\mathbf{N}_2 \\ &= -|\Omega_1|\mathbf{N} - |\Omega_2|\mathbf{N}_2 \end{aligned} \tag{5}$$

by the divergence theorem. From (2), (3), and (5) we obtain

$$\left(|\Sigma_1| \sin\gamma_1 + 2H|\Omega_1|\right)\mathbf{N}_1 + \left(|\Sigma_1| \sin\gamma_2 + 2H|\Omega_2|\right)\mathbf{N}_2 = 0. \tag{6}$$

Since $\mathbf{N}_1$ and $\mathbf{N}_2$ are independent, we are led to

Theorem 2.1 *A tubular bridge can exist in a wedge only if*

$$|\Sigma_1| \sin \gamma_1 + 2H|\Omega_1| = 0, \qquad |\Sigma_2| \sin \gamma_2 + 2H|\Omega_2| = 0. \tag{7}$$

In these relations, the sign of H is determined by our convention that $\mathbf{N}$ is directed exterior to $\mathcal{S}$. Thus (for example) H would be negative for a convex surface. The theorem yields immediately

Corollary 2.1 *There is no tubular bridge in a wedge, for which $H > 0$.*

Corollary 2.2 *There is no tubular bridge in a wedge, for which $H \neq 0$ and with contact angles 0 or π on the bounding walls.*

If the planes are parallel, then the identical proof yields

Corollary 2.3 *If a tubular bridge meets parallel planes in simple curves Σ_1, Σ_2 and makes constant angles γ_1, γ_2 with the planes, then*

$$|\Sigma_1| \sin \gamma_1 + 2H|\Omega_1| = |\Sigma_2| \sin \gamma_2 + 2H|\Omega_2|. \tag{8}$$

Suppose now that the two planes Π_1, Π_2 are initially parallel. Then *any tubular liquid bridge of constant mean curvature that meets Π_1 and Π_2 with constant contact angle on each plane is rotationally symmetric and intersects any intermediate parallel plane Π transversally in a circle.* This follows from a procedure due to Wente [39], who adapted the Aleksandrov reflection method to the case of drops on a single planar surface. The procedure applies in the identical way to the case of two parallel planar surfaces considered here.

Let us denote by r the radius of the circle in the plane Π and by Ψ the angle between Π and $\mathcal{S}$ along that circle. Applying Corollary 2.3 with Π in place of Π_2 we obtain $\sin \Psi + Hr =$ constant (independent of Π). But if (7) holds on either plate then the constant vanishes, and we conclude that the bridge is spherical. We have proved the following result, originally conjectured by Concus and Finn [9]:

Theorem 2.2 *Suppose that a tubular bridge between two parallel plates is initially not a sphere. Then the configuration changes discontinuously on infinitesimal tilting of one of the plates, in the sense that either no tubular bridge exists for the tilt, or else that at least one of the quantities Σ_j, Ω_j, H must change discontinuously.*

In this result, the former eventuality is not empty. McCuan [25] proved that if the data γ_1, γ_2 do not admit a spherical surface as a tubular bridge in a wedge of opening 2α, then no embedded tubular bridge exists. But a necessary condition for a spherical bridge is

$$\gamma_1 + \gamma_2 - 2\alpha > \pi. \tag{9}$$

Thus, *if the resultant data after tilting do not satisfy* (9), *then the tilt leads either to disappearance of the configuration* (*perhaps by flow along the edge*) *or else to a change of topological type for the surface.* We take up this matter further in the following section.

We note that the hypothesis of embeddedness is essential; an extension of Wente's construction in [40] provides examples of immersed bridges between the planes of a wedge. Clearly, the assumption of constant contact angle is essential. Assuming that any equilibrium satisfies a constant contact angle condition, however, the proof shows that no nearby equilibrium exists for a certain range of constants.

3 Observations

We consider the question, as to what happens physically to a tubular liquid bridge of prescribed volume between parallel plates, making prescribed contact angles with the plates, when one or both of the plates is tilted. If one permits change of topological type, then a non countable infinity of choices is available, in which parts of the volume go into spherical drops having no contact with the plates, other parts go into drops contacting only one of the plates, and still other parts may go into drops in the wedge, wetting a segment of the intersection line L. In what follows, we will restrict attention to connected liquid masses, in

a wedge of given opening $0 < 2\alpha < \pi$. We then find, by the same argument used by Wente in [39], that there are no "holes" (air bubbles) contained within the masses; that is, the planar contact regions Ω_1 and Ω_2 are simply connected and the second homology group of the fluid mass vanishes. In all cases in which $0 < \gamma_1, \gamma_2 \leq \pi$, a spherical cap contacting only one of the Π_j (the other plane being contacted in a vacuous sense) is a conceivable configuration for any volume, and provides a local energy minimum. We show below in Sec. 4 however that the drop in the wedge (which we denote by *edge blob*) and the tubular bridge are mutually exclusive events, and we will indicate how continuous change of boundary data can lead from a tubular bridge to an edge blob, and then either to disappearance along the edge to infinity or to a drop contacting only one plate.

We return first to the question of what happens with initial tilt. In particular cases, there is an immediate answer as to presumed behavior:

Theorem 3.1 *If the initial configuration is spherical, then continuous change to a new spherical configuration is always possible.*

Proof: Following (small) tilting of the plates, we translate the initial sphere in a direction orthogonal to one of the plates until the desired contact angle with that plate is restored, then slide it along that plate until it makes the prescribed contact angle with the other plate. Following those motions, the prescribed volume can be restored without changing contact angles, by a dilation relative to a point on the intersection line of the plates. Since each of these motions can be made to be vanishingly small with the amount of tilt, the resultant of the three of them has the same property. □

The situation just described is exceptional, in the sense that for a bridge between given parallel plates with given contact angles there is exactly one volume for which the liquid will assume a spherical shape; since stable drops of arbitrarily large volume can be found for any contact angles, we see that the case covered by Theorem 3.1 is a rare event among the set of

possible physical bridges. In all other cases, the change with tilting must be discontinuous. We find the following behavior:

Theorem 3.2 *Suppose that for an initial non-spherical bridge configuration between parallel plates, there holds $\gamma_1 + \gamma_2 > \pi$. Then a jump to a spherical tubular configuration between the plates is possible. If initially $\gamma_1 + \gamma_2 < \pi$ then no tubular bridge can result from sufficiently small tilting. In neither case can infinitesimal tilting lead to an edge blob (finite or infinite) which admits a local representation near the intersection with L as a graph over a plane orthogonal to L.*

Proof: In the first case, (9) holds for α small enough, so that a spherical bridge exists. In the latter case, (9) fails for α small enough, thus excluding a spherical bridge. By McCuan's theorem [25] if there is no spherical bridge then there is no tubular bridge. In both cases, an edge blob with representation as indicated would contradict Theorem 3 of [8]. □

Thus, in either of the two eventualities contemplated in the theorem, it cannot be expected that an edge blob will appear immediately on tilting, as the result of discontinuous change. In the first case however, if a spherical bridge is obtained after an infinitesimal tilt and the opening angle 2α is increased until $\gamma_1 + \gamma_2 < \pi + 2\alpha$, then the bridge should transform smoothly to an edge blob in the wedge with spherical surface interface; see Theorem 4.1 below and the continuing discussion in the Case 1^- further down.

The exclusion of an edge blob in this result holds without growth hypotheses in the representation. The result suggests strongly that in the latter case an infinitesimal tilt will lead to disappearance of the fluid along the edge to infinity. This view is further supported by the considerations that follow.

4 Configurations

We seek to determine what configurations can occur in a wedge of given opening 2α, in terms of boundary data. We take as starting point the result of [8], that a necessary condition for

tangent plane to $\mathcal{S}$ continuous to the vertex is that the data γ_1, γ_2 lie in the closed rectangle $\mathcal{R}$:

$$\begin{aligned} \pi - 2\alpha \leq \gamma_1 + \gamma_2 \leq \pi + 2\alpha \\ 2\alpha - \pi \leq \gamma_1 - \gamma_2 \leq 2\alpha + \pi \end{aligned} \tag{10}$$

inscribed in the square $Q_\gamma : 0 \leq \gamma_1, \gamma_2 \leq \pi$ of permissible data, or equivalently that the cosines $B_1 = \cos\gamma_1$, $B_2 = \cos\gamma_2$ lie in the closed ellipse $\mathcal{E}$:

$$B_1^2 + B_2^2 + 2B_1B_2\cos 2\alpha \leq \sin^2 2\alpha \tag{11}$$

inscribed in the square $Q_B : -1 \leq B_1, B_2 \leq 1$ of admissible data (Figure 2). We note that the boundaries of these inscribed regions correspond to vertical tangent planes at the vertex (relative to a coordinate system in which L is vertical), and that interior to the regions the tangent planes are not vertical.

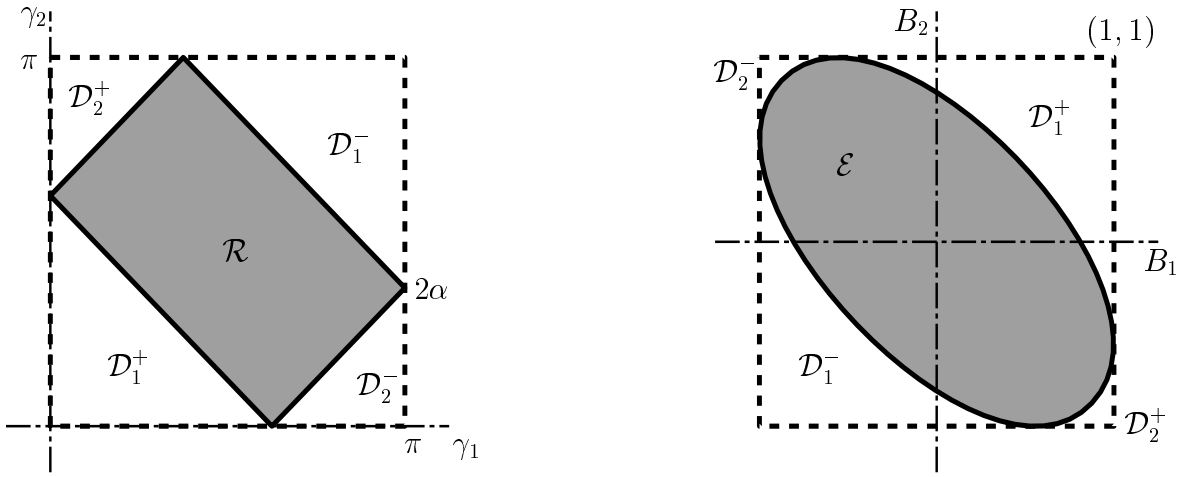

Figure 2: Rectangle and ellipse of data for smoothness

Points interior to the shaded regions of Figure 2 provide data for which solutions of (1) with continuous tangent plane up to L actually exist, for any prescribed $H > 0$. Such solutions can be obtained explicitly as the spherical surfaces $\mathcal{S}$ of portions of balls of radius

$1/H$ cut off by the wedge. In fact, given α, B_1, B_2 with $(B_1, B_2) \in \mathcal{E}$, we may determine θ_0 and $k > 0$ from the relations

$$k = \frac{\sin(\alpha + \theta_0)}{-B_1} = \frac{\sin(\alpha - \theta_0)}{-B_2}\,. \tag{12}$$

A sphere of arbitrary radius kr_0, whose center is positioned at $(r_0 \cos\theta_0, r_0 \sin\theta_0)$ in a coordinate plane orthogonal to L whose positive x-axis bisects the wedge with origin at the vertex, then provides a surface $\mathcal{S}$ with the requisite property. We note that the relation (11), which is necessary for a spherical solution, implies $k \geq 1$.

The following result provides an extension of the theorem of H. Hopf, that every genus zero immersion of a closed surface of constant mean curvature is a sphere.

Theorem 4.1 *For data interior to $\mathcal{E}$ (or $\mathcal{R}$), the spherical surfaces $\mathcal{S}$ determined by* (12) *are the unique surfaces with local representation near L as a graph over a plane orthogonal to L, that satisfy the contact angle conditions interior to the planes.*

This result is proved in detail in [13], where somewhat weaker conditions are formulated. The conditions do not require a globally embedded surface. In view of the particular interest of the result in the present context, we outline here the proof.

By a theorem of Concus and Finn [6], the surface is bounded at L in a local representation with L as vertical axis. By a theorem of Simon [31], $\mathcal{S}$ has continuous tangent plane to L, and by results of Miersemann [27] and of Lieberman [23] the unit normal to $\mathcal{S}$ is Hölder continuous to L. Corresponding to the given data, the tangent plane at the vertex meets the wedge plates in the tangent lines to the trace of $\mathcal{S}$ on the plates. These lines meet each other in the angle β determined by

$$\sin^2 2\beta = \frac{\sin^2 2\alpha - (B_1^2 + B_2^2 + 2B_1B_2\cos 2\alpha)}{(1 - B_1^2)(1 - B_2^2)} \tag{13}$$

which according to (11) is positive for all data interior to $\mathcal{E}$.

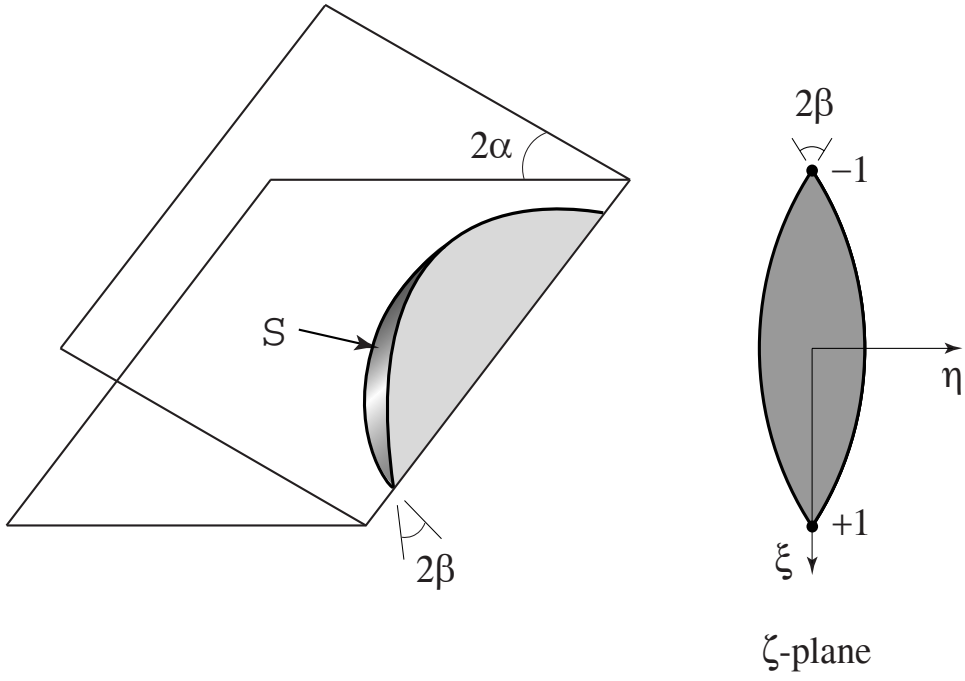

Figure 3: Edge blob and mapping of $\mathcal{S}$ to lens domain

The indicated trace is assumed smooth except at the vertices. We map $\mathcal{S}$ conformally onto a lens domain in the ζ-plane as shown in Figure 3, keeping the angles at the vertices unchanged. Composition of this mapping with the mapping

$$Z = \log \frac{\zeta - 1}{\zeta + 1} \tag{14}$$

takes $\mathcal{S}$ to an infinite horizontal strip in the Z-plane, of height 2β.

By hypothesis, $\mathcal{S}$ meets the plates in constant angles γ_1, γ_2. Since the plates are planar, the intersection curve C is a curvature line on the plates (i.e., every curve on a plane is a curvature line). By a theorem of Joachimsthal [20], C is also a curvature line on $\mathcal{S}$. But the image of C in the Z-plane consists of two coordinate lines. It follows that if l, m, n are the coefficients of the second fundamental form in the Z-plane, then $m = 0$ on the boundary of the strip.

By the local smoothness shown just above, in local Euclidean coordinates the position

vector $\mathbf{x}$ has Hölder continuous first derivatives up to each vertex V. Consequently the coefficients of the associated Beltrami system for the mapping to the lens are Hölder continuous, and we conclude that $\mathbf{x}$ has Hölder first derivatives up to the vertices in the lens plane. Using results of Siegel [30], Gerhardt [17, 18], Ural'tseva [34] (see [10, p. 210, Note 5] and a theorem of Azzam [2], we find that

$$|D^2\mathbf{x}| = o(\rho^{-2}), \tag{15}$$

in the ζ plane, ρ being distance from a vertex. Hence the coefficients L, M, N of the second fundamental form in the ζ plane are also $o(\rho^{-2})$ at the vertices.

Since $|d\zeta/dZ| = O(\rho)$ at the vertices and since the Codazzi equations for a surface of constant mean curvature imply that $(L - M) - 2iM$ is analytic on the surface and that

$$[(L - N) - 2iM]\, d\zeta^2 = [(l - n) - 2im]\, dZ^2, \tag{16}$$

we obtain from (15) that $(l - n)$ and m tend to zero at infinity in the strip. But m is harmonic and vanishes on the boundary, and there follows $m \equiv 0$. Hence $(l - n)$ is constant, and since it approaches zero at infinity, it vanishes identically. We conclude that $\mathcal{S}$ is totally umbilic, and hence $\mathcal{S}$ is spherical, as was to be shown. $\square$

We examine now what happens as the boundaries of $\mathcal{E}$ (or of $\mathcal{R}$) are approached from within the domain, for a fluid mass of prescribed volume. (Note that, in contrast to the case of parallel plates, volume in a wedge is an inessential parameter: any positive volume can be obtained from any other positive volume by similarity, without affecting the data.) The limiting tangent planes at the vertices are vertical and thus contain the intersection line L. We denote by $\mathcal{L}_j^{\pm}$ the curves adjacent to $\mathcal{D}_j^{\pm}$, and distinguish the possible configurations:

Case 1^-; Data on $\mathcal{L}_1^-$: This case is indicated in Figure 4, and from a formal point of view presents no singularity. Here, (9) is replaced by $\gamma_1 + \gamma_2 = \pi + 2\alpha$. A further motion into the domain $\mathcal{D}_1^-$ yields data for which (9) holds, and corresponding tubular bridges with spherical boundaries appear. The relation (12) then ceases to yield a blob contacting L.

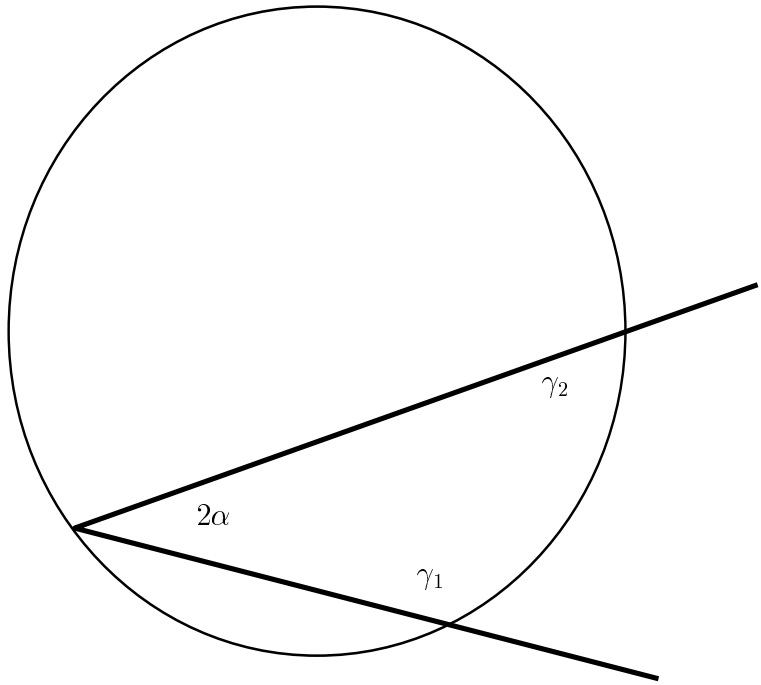

Figure 4: Limiting configuration; $\gamma_1 + \gamma_2 = \pi + 2\alpha$

Beyond that, it follows from Theorem 3 *of* [8] *that no solution, spherical or not, can exist even locally as a graph over a plane orthogonal to L. This result holds irrespective of growth conditions as L is approached.*

Case 1^+; Data on $\mathcal{L}_1^+$: The limiting configuration is a sphere of infinite radius that passes through the vertex, as indicated in Figure 5. In order to preserve volume, the liquid has spread out to infinity in the edge. If data are assigned from $\mathcal{L}_1^+$ or from $\mathcal{D}_1^+$, (12) will again fail to yield a spherical solution surface meeting the planes in the prescribed angles, nor can any edge blob exist that is locally a graph near L.

Case $2^\pm$; Data on $\mathcal{L}_2^+$ or $\mathcal{L}_2^-$: A limiting spherical configuration exists, as indicated in Figure 6, but does not cover a neighborhood of V; it is perhaps better interpreted as a drop resting on a single plane, making the prescribed angle with that plane (this entails a discontinuous change in the formally contemplated boundary condition). For data points

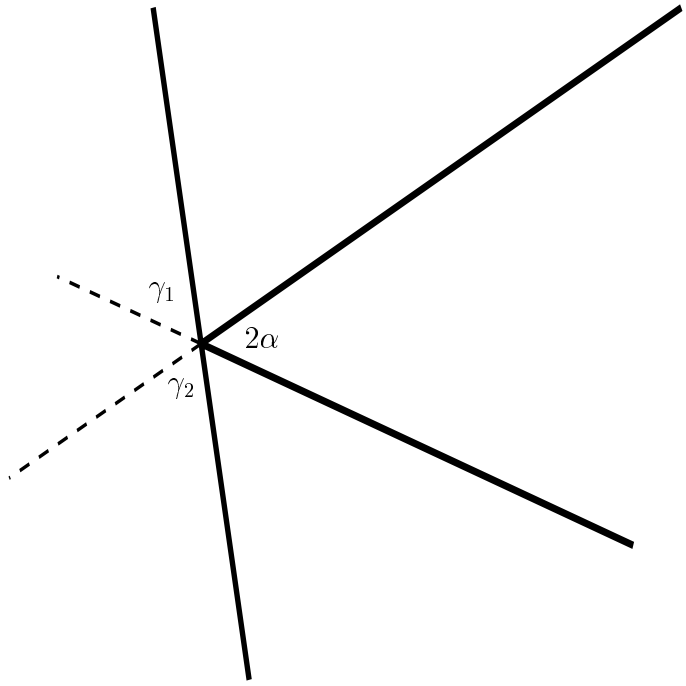

Figure 5: Limiting configuration; $\gamma_1 + \gamma_2 = \pi - 2\alpha$

interior to $\mathcal{L}_2^{\pm}$, the tangent plane at V enters the wedge region; thus it is clear that no drop of the stated (edge blob) form can exist, with unit normal continuous up to V. Further, data from $\mathcal{D}_2^{\pm}$ yield formally according to the relations (12) a drop contacting one of the bounding plates Π_j exterior to the wedge region (see Figure 7), and which therefore cannot be realized physically. We can however regard the drop as a spherical cap lying entirely on one of the planes, having no contact with the other plane, neglecting the portion that extends exterior to the wedge. This drop appears geometrically as a continuous transition from the originally contemplated drops meeting both planes.

The results just described are outlined in Figure 8, which envisages motions along the two principal diagonals of the squares Q_γ or Q_B of admissible data. The surfaces illustrated were computed by means of the Surface Evolver program of K. Brakke [3]. Although a more exotic behavior has not been completely excluded by our discussion, the evidence seems

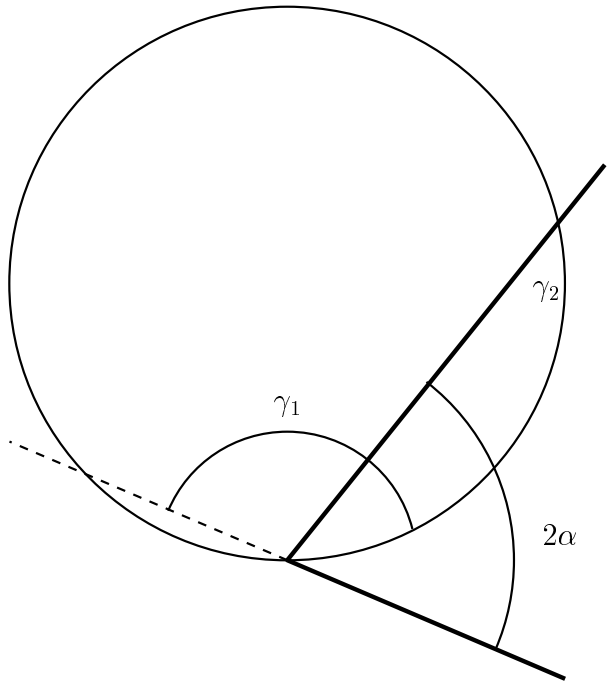

Figure 6: Limiting configuration; $\gamma_1 - \gamma_2 = \pi - 2\alpha$

strong that the configurations described are those that will be encountered under ordinary physical conditions. Note especially that for data in $\mathcal{R}$ near $\mathcal{D}_2^{\pm}$, the drop nearly unwets one of the plates, so that there is a continuous transition on leaving $\mathcal{R}$ into a spherical cap resting on a single plate (although the formal solution of (12) becomes physically unrealistic). See, however, the discussion in the next following section.

5 Discussion

As noted just above, for data in $\mathcal{D}_2^{\pm}$ we have not completely excluded the occurrence in wedges of non-spherical blobs, having discontinuous normal vector where the surface meets the edge. In Theorem 4.1 above, we showed under some restrictions that for data in $\mathcal{R}$ all such drops are spherical, and indeed spherical blobs can be found explicitly from (12)

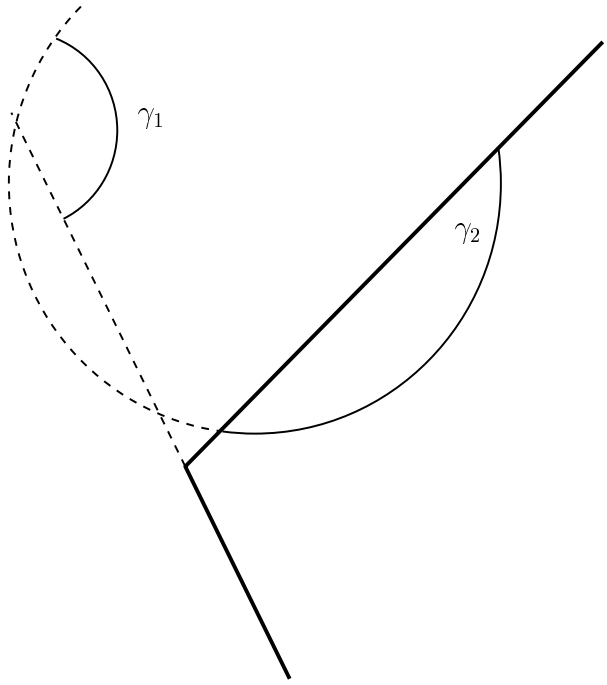

Figure 7: Data in $\mathcal{D}_2^-$

for such data. With $\mathcal{D}_2^\pm$ data however, the indicated exotic behavior can actually occur for capillary surfaces $u(x, y)$ that wet an edge. Such surfaces were initially calculated by Concus and Finn [9] in containers whose walls consist of portions of circular cylinders of prescribed radius meeting in an edge; the existence of these surfaces was later proved by Finn [12]. An example that fits more precisely into the present context is that of a vertical cylinder having square base domain, with $\mathcal{D}_2^\pm$ data on the symmetry line $\gamma_1 + \gamma_2 = \pi$, and with γ_1, γ_2 interchanged on adjacent walls. This model leads always to a minimal surface; it was studied from a computational point of view by Mittelmann and Zhu [28]. We support the calculations of those authors by showing that solutions actually exist in the cases they consider. We shall present in fact a much more general result. We note first that for surfaces

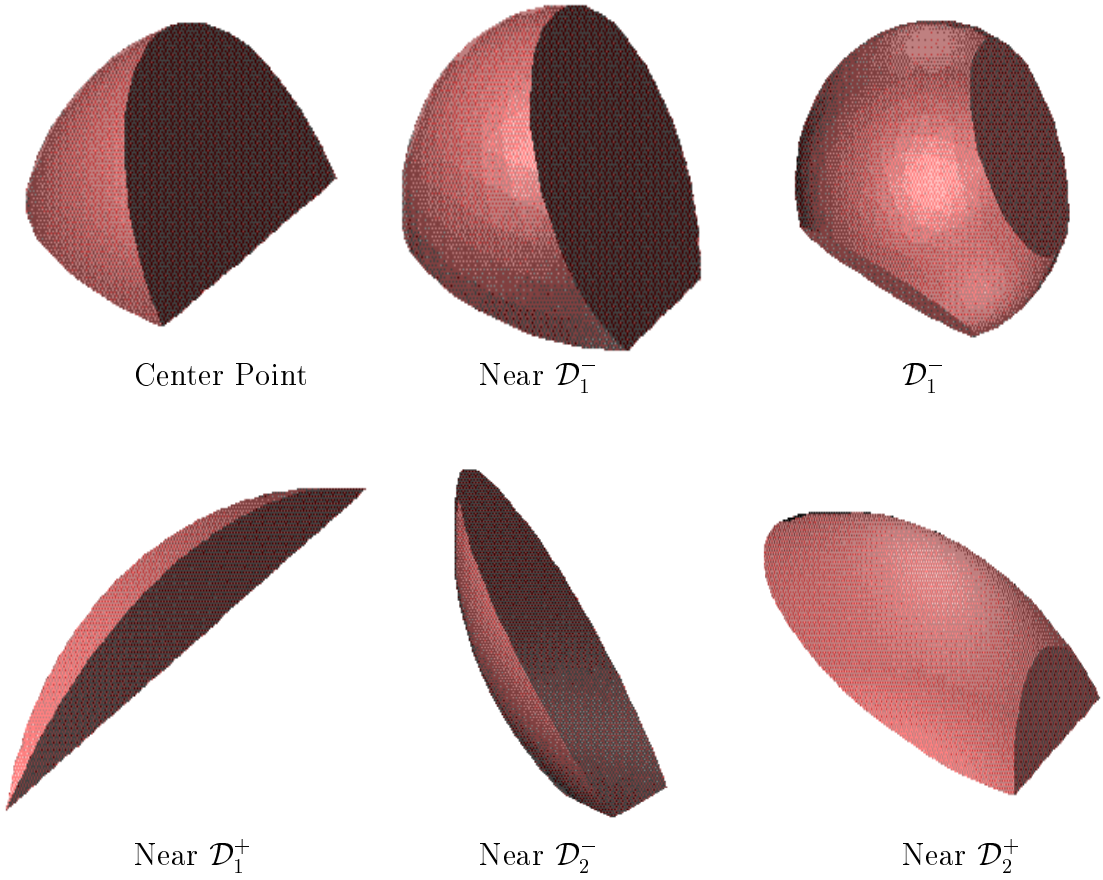

Figure 8: Representative configurations for varying contact angle data.

that are graphs $u(x, y)$ over a base domain Ω, (1) can be given the scalar form

$$\operatorname{div} Tu = 2H, \qquad Tu = \frac{\nabla u}{\sqrt{1 + |\nabla u|^2}} \tag{17}$$

while for contact angles constant on generators of the cylindrical boundary walls Z the contact angle boundary condition becomes

$$\nu \cdot Tu = \cos \gamma \tag{18}$$

on $\Sigma = \partial\Omega$. Here ν is exterior unit normal on Σ. We consider, as in [28], a domain Ω which is a unit square, and prescribe data γ_1 on two opposite sides, and data γ_2 on the remaining two

sides. Note that no data is prescribed at the corners, nor is any growth condition imposed at those points.

Theorem 5.1 *Let Ω denote the square $0 \le x \le 1$, $0 \le y \le 1$, let $(\gamma_1, \gamma_2) \in (\bar{\mathcal{R}} \cup \bar{\mathcal{D}}_2^- \cup \bar{\mathcal{D}}_2^+)$. Then there exists a unique (up to additive constant) solution $u(x, y)$ of (17), (18), such that the data γ_1, γ_2 are achieved on successive sides, as indicated.*

We prove the theorem in the Appendix. Note that the result is sharp, in the sense that there can be no solution for data in $\mathcal{D}_1^{\pm}$. We observe that for data in $\mathcal{D}_2^{\pm}$, the solution surface cannot be spherical, as its unit normal vector is discontinuous at the corner. The surface is however bounded, as follows from Theorem 7.3 of [5], or Proposition 1 of [21]. Let us reflect the surface in a horizontal plane, and lower the reflected surface rigidly until it lies entirely below the original one. The region interior to the cylinder Z and bounded between the two surfaces can be regarded as a liquid blob that wets the four edges of the support cylinder, with the same contact angles γ_1, γ_2. Thus, by introducing two further support surfaces beyond those of the two forming the original wedge, blobs appear with very different behavior at the edge than is encompassed in the discussion of Sec. 4.

This result shows in particular, that *for data in $\mathcal{D}_2^{\pm}$ it is not possible to exclude exotic behavior at the edge by local considerations.* There is an apparent connection with the vertex theorems for drops on support surfaces, introduced in [13]. The liquid blob in a global wedge consisting only of two planes has two vertices; the blob just constructed has nominally eight vertices, however we may view the configuration alternatively (cf. Theorem 4 of [13]) as a semi-infinite blob filling out the cylinder on one side of the surface, in which case we find four vertices.

In the light of this discussion and of that in Sec. 4, we make the

Conjecture *The free surface of any liquid blob in a wedge (that is, drop with just two vertices) which makes constant contact angles with each of the two wedge faces, is metrically spherical.*

For data (contact angles) arising from $\mathcal{R}$ the conjecture is proved in Theorem 4.1 above, at least for surfaces that are locally graphs near L; it remains true in this case even if there are three vertices, see Theorem 4 in [13]. Subject to the same restriction, the result holds vacuously for data in $\mathcal{D}_1^{\pm}$, as no blob can then exist ([8, Theorem 3]). The case of principal interest that remains unsettled is that of data from $\mathcal{D}_2^{\pm}$; the example discussed just above shows that the hypothesis on number of vertices is necessary.

6 Energy considerations

It follows from the isoperimetric inequality that, in the absence of gravity and of contact with boundary surfaces, a spherical connected drop without holes has less surface energy than any other configuration of the same volume. From a procedure of Gonzalez [19] we find that a spherical cap resting on a plane with prescribed contact angle γ has less energy than any other configuration of the same volume, for which each component meets the plane (if at all) in angle γ, and no other rigid boundary is present. This result holds both in "wetting" ($\gamma < \pi/2$) and in "non-wetting" ($\gamma \geq \pi/2$) configurations. (Under restriction to spherical free surfaces, the result was anticipated by Reynolds and Satterlee [29].) Here the mechanical energy E is the sum of free surface energy $F = \sigma S$ and wetting energy $W = -\sigma A \cos\gamma$, where σ is the surface tension, S the free surface area and A the wetted area. Our further considerations rest on the following general observations, that seem to have been overlooked in existing literature.

Let us assume that a sphere Σ cuts off an area $\mathcal{W}$ from a surface $\mathcal{Z}$ and bounds with $\mathcal{W}$ a volume V inside the ball bounded by Σ. Let $\mathbf{x}$ be the position vector in $\mathbb{R}^3$ measured from the center of Σ, $\mathbf{n}$ the unit normal to $\mathcal{W}$ at $\mathbf{x}$ that points out of V, and $\gamma_{\mathbf{x}}$ the angle between $\mathbf{n}$ and the outward unit normal to Σ along the circle where the tangent plane to $\mathcal{W}$ at $\mathbf{x}$ and Σ intersect. One then has the relation

$$\mathbf{x} \cdot \mathbf{n} = -\cos\gamma_{\mathbf{x}}.$$

We now integrate $\operatorname{div} \mathbf{x}$ over V and apply the divergence theorem. In view of the relation just above, one obtains

Lemma 6.1

$$-\int_{\mathcal{W}} \cos \gamma_{\mathbf{x}} \, d\omega_{\mathbf{x}} + |\mathcal{S}| = 3|V|.$$

In the configuration described above, assume that $\mathcal{Z}$ consists of countably many planes Π_j that meet the sphere Σ of radius R in angles γ_j (measured within V) and have portions $\mathcal{W}_j$ on ∂V. In this situation we have

Corollary 6.1

$$-\sum |\mathcal{W}_j| \cos \gamma_j + |\mathcal{S}| = 3|V|,$$

and the energy of such configurations is given by

$$E = \frac{3\sigma|V|}{R}.$$

In particular, the mechanical energy of any such configuration is positive.

We are now prepared to prove

Theorem 6.1 *If a spherical bridge or edge blob in the absence of gravity meets two wedge faces in angles γ_1, γ_2, then that configuration has smaller mechanical energy than does any connected liquid mass of the same volume that meets only one of the faces in the prescribed angle for that face.*

Proof: In view of the above result of Gonzalez, it suffices to restrict attention to the cases in which both configurations are spherical. A typical configuration in which the liquid contacts both plates is illustrated in Figure 9. In this case, we translate one of the plates along the the extension of the other while keeping its normal fixed. Simultaneously, we decrease R so that the volume bounded by the sphere and included between the two planes remains constant. According to Corollary 6.1 the energy of the resulting configurations increases

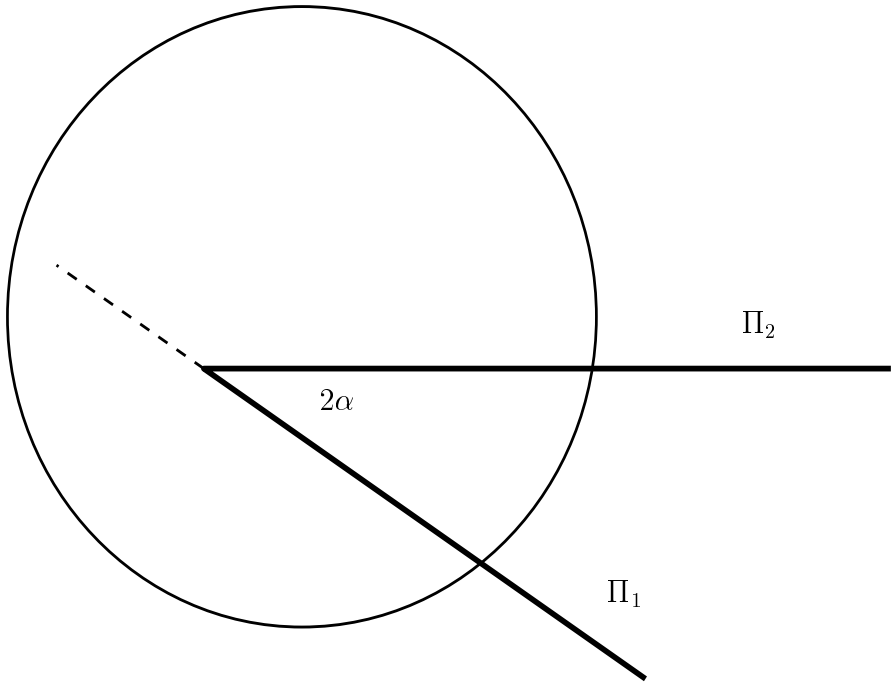

Figure 9: Liquid contacting two plates.

until the translated plane no longer contacts the sphere. The terminal configuration is that of a single spherical drop on a single plate and, thus, the stated result is obtained. □

We observe that in the proof of Theorem 6.1 the contact angle on the translating plate decreases monotonely during the procedure. We thus obtain the following:

Corollary 6.2 *In any blob or bridge configuration of given volume, the mechanical energy is a monotone decreasing function of each of the two contact angles.*

We consider now a spherical blob or wedge bridge configuration, of given volume and prescribed contact angles, and examine the dependence of mechanical energy on the angle 2α between the bounding plates. In the case of a bridge (data in $\mathcal{D}_1^-$), one sees immediately that *the energy is independent of* α. The situation for blobs is described by Theorem 6.2 below.

Recall that spherical blobs are obtained for data in $\mathcal{R}$ and, in a degenerate sense, for data on the segment $\{(\gamma_1, \gamma_2) : \gamma_1 + \gamma_2 = \pi + 2\alpha;\ \gamma_1, \gamma_2 < \pi\}$. We consider such a blob in a wedge of opening angle 2α and distinguish three subcases:

Theorem 6.2 *1.* $\gamma_1 + \gamma_2 > \pi$.

In this case, α *can be decreased to zero and there is a family of corresponding configurations that transform the original configuration smoothly to that of a spherical bridge, with the same volume and contact angles, between parallel planes. During this transformation, the mechanical energy decreases monotonely until* $\gamma_1 + \gamma_2 = \pi + 2\alpha$*, which is the transition point between blob and wedge configurations; for further decrease of* α *the energy remains constant.*

2. $\gamma_1 + \gamma_2 < \pi$.

In this case, α *can be decreased down to but not including the value* $\alpha_c = [\pi - (\gamma_1 + \gamma_2)]/2$*. In this procedure the energy decreases monotonely to zero and the drop spreads out along the intersection line* L *of the two planes. More precisely, the length* l *along* L *included in the boundary of the drop is such that* $l(\alpha - \alpha_c)^{1/3}$ *is bounded above and below by positive constants, and the entire drop is contained in a cylinder with axis* L *and radius* r *with* $r(\alpha - \alpha_c)^{-1/6}$ *bounded above and below by positive constants. For further decrease of* α*, no spherical configuration is possible.*

3. $\gamma_1 + \gamma_2 = \pi$.

In this case, α *can be decreased down to but not including zero with correspondig configurations whose energy decreases monotonely to zero. The drop spreads out both along the intersection line* L *and out into the wedge. More precisely as* α *approaches zero, the interface is contained in an* ϵ*-neighborhood of a circular arc* C_α *in one of the plates with* $\epsilon\alpha^{-2/3}$ *bounded above and below by positive constants. The circular arc* C_α*, which is the intersection of the spherical interface with that plate, encloses an area*

A on that plate with $A\alpha^{2/3}$ bounded above and below by positive constants, and C_α converges, when rescaled to unit radius, to a semicircle.

Proof: Case 1. We start with a spherical blob $\mathcal{S}$ in a wedge between planes Π_1 and Π_2. See Figure 10 where the dark lines represent the initial position of the planes and the initial spherical surface Σ is indicated by an equatorial circle in the plane of the figure. We may assume that $\gamma_1 > \pi/2$ so that the wedge region lies on the same side of Π_1 as the center of the sphere. Since $\gamma_2 > \pi - \gamma_1$, either Π_2 is closer to the center of Σ as indicated in the figure,

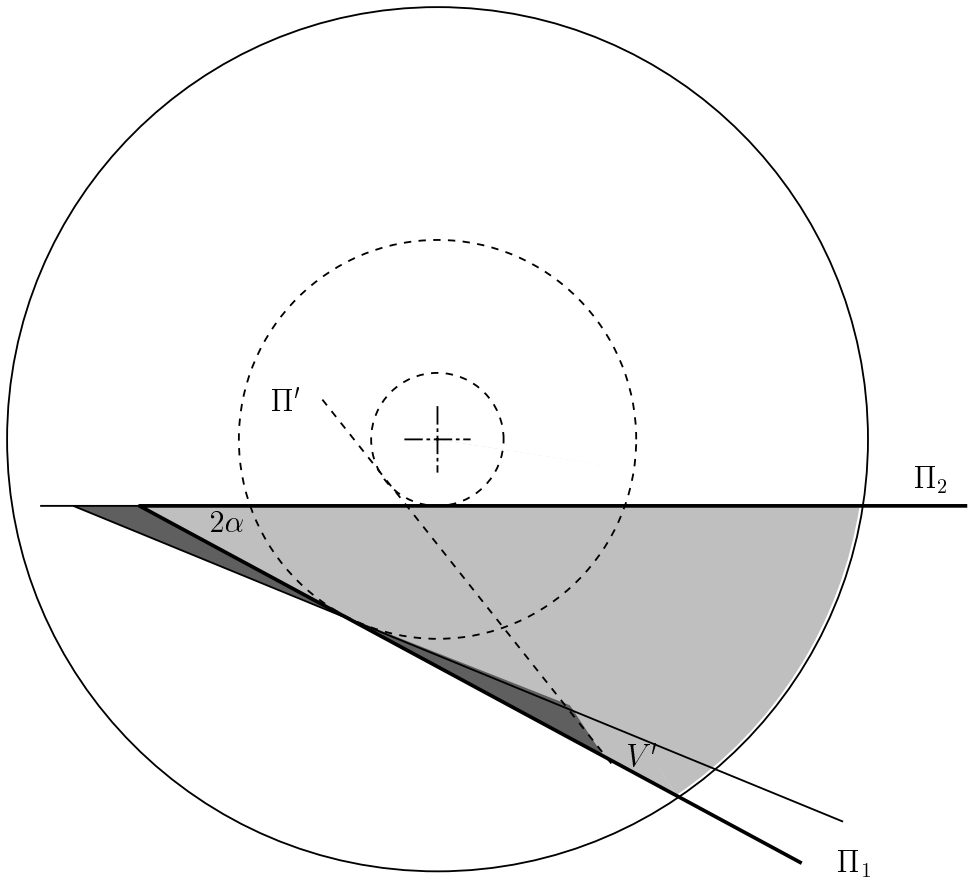

Figure 10: Proof of Theorem 6.2.

or the center of the sphere lies interior to the wedge region. Such a blob can be transformed

to any bridge with the same contact angles and volume as follows. We first roll one of the plates around a cylinder with axis through the center of $\mathcal{S}$ and orthogonal to the plane of the figure so that the wedge opening 2α decreases and the intersection line L moves closer to the equatorial circle.

One observes that the volume enclosed by the sphere and between the resulting plates is then less than the original volume. In fact, if Π' is an auxiliary plane placed as indicated in Figure 10 so that the dark shaded triangles are congruent, then the volumes in the sphere that project onto the shaded triangles are equal, and there is an additional volume V' that is removed as a result of the motion. This volume can be restored by a dilation centered on L which increases the radius of the sphere. The resulting energy according to Corollary 6.1 has decreased.

Since the enclosed volume stays bounded from zero, the radius of the spherical interface increases to a finite limit R. The reasoning above shows that the energy is an increasing function of the wedge angle until the distance from the intersection line L to the center of the sphere equals R. At this point, L reaches the equatorial circle and becomes tangent to the sphere, and the topology of the edge blob changes to that of a bridge. Any continued rolling of the support plane, which decreases the wedge angle and leaves the contact angles constant as before, results in bridge configurations with the same energy and volume. Since any wedge configuration that admits a spherical tubular bridge can be obtained in this way, the result follows.

Case 2. In this case, we may assume that the distance from the center of Σ to Π_2 is greater than that from the center to Π_1, and that the center of Σ lies in the half space determined by Π_2 opposite that containing the enclosed volume. See Figure 11.

One sees now directly that decreasing α by rolling one of the planes as before decreases the volume. Hence, when the volume is corrected by a dilation, the overall energy decreases as before. In this case, however, there is no positive lower bound for the volume that can be

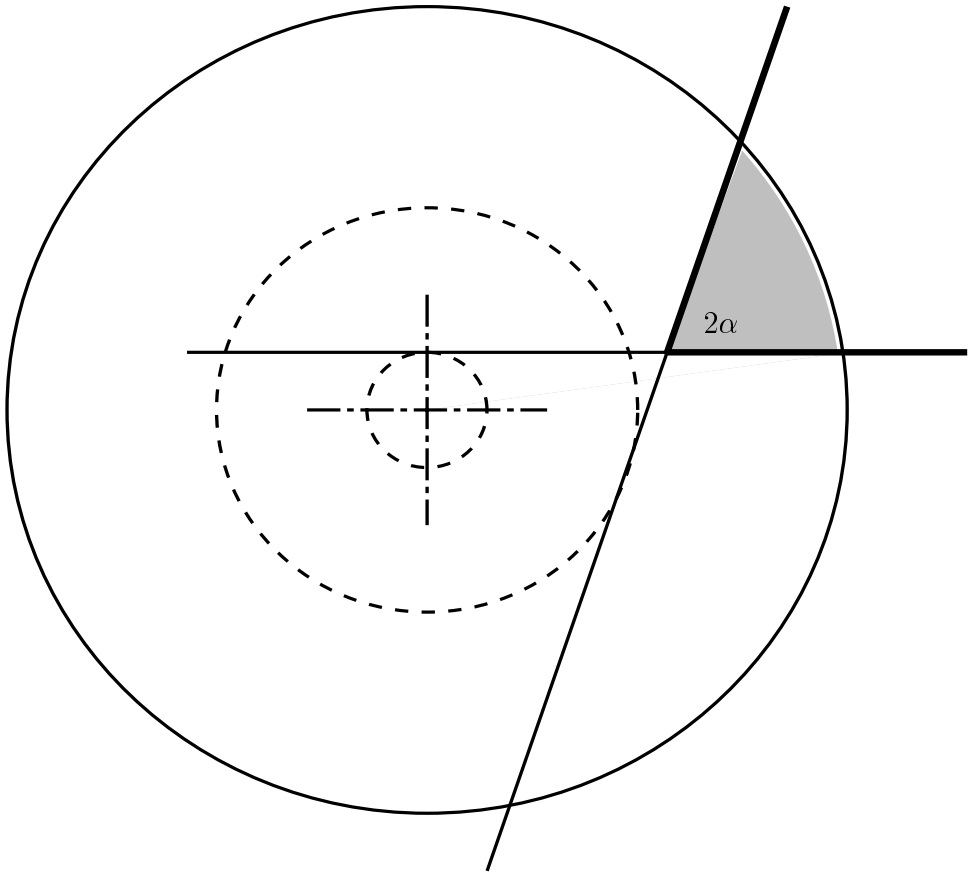

Figure 11: Proof of Theorem 6.2, Case 2.

obtained by rolling, so that the radius of the interfaces becomes arbitrarily large. The angle α is bounded below by the value given in the statement of the theorem, and it follows from this that the drop tends, as a set, to the intersection line L.

The order of magnitude estimates in the theorem are obtained easily by observation of the limiting geometrical configuration.

Case 3. In this case, Π_1 and Π_2 are equidistant from the center of Σ, and the center of Σ may be assumed to be on the same side of Π_1 as the enclosed volume, but on the opposite side of Π_2 as the enclosed volume; see Figure 12.

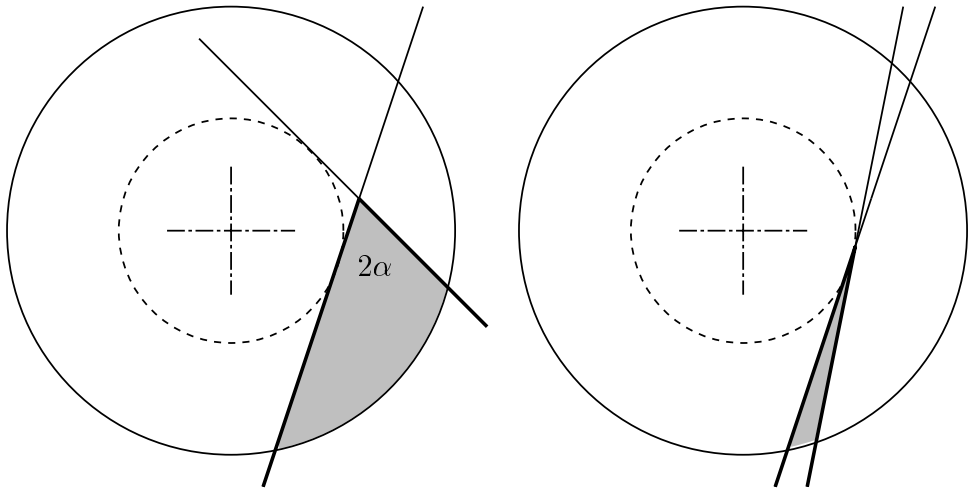

Figure 12: Proof of Theorem 6.2, Case 3.

As α is decreased by rolling one of the planes on a cylinder as before, the intersection line L approaches a point on the cylinder. The rolling again results in arbitrarily small volumes which must be accompanied by arbitrarily large dilations to correct the volume. It follows from Corollary 6.1 that the energy tends to zero. The order of growth estimates and goemetric statements can be ascertained from the limiting configuration indicated in Figure 12. It is also clear that explicit estimates could be obtained.

The order of magnitude estimates follow analogously as in Case 2. □

Thus, *the energy of any bridge of given volume is less than that of any blob with the same contact angles on the plates, and the energy of the blob is in turn less than that of any drop on a single plate that meets the plate in either of the prescribed angles.*

It is interesting that in Case 2 every finite point in the wedge away from L is eventually no longer in contact with the drop as α decreases to its critical value while, in contrast, in the borderline Case 3 every finite point in the wedge is eventually on the boundary of the drops that result as the wedge angle is decreased. The perturbation from Case 3 to Case 2, as the radii of the contact circles separate from each other, is thus seen to be singular in the

limit as the blob radius becomes infinite.

We were informed by Henry Wente that alternate proofs of Theorems 6.1 and 6.2 can be obtained by adapting procedures from [42]. It may also be possible to obtain a proof from the methods of [46], though the energy considered there, being a *parametric elliptic functional*, is essentially different from the energy considered in this paper.

Acknowledgments. We wish to thank Victor Brady for carrying out the computations leading to Figures 8. This research was supported in part by a grant from the National Aeronautics and Space Administration, and in part by a grant from the National Science Foundation. The second and third authors wish to express their thanks to the Max-Planck-Institut MIS in Leipzig for its hospitality during completion of the work.

Appendix: Proof of Theorem 5.1

Our essential weapon will be Theorem 7.10 of [10]. Since H is constant in our setting, the problem reduces to showing that for every Caccioppoli set $\Omega^* \subset \Omega$, with $\Omega^* \neq \Omega, \emptyset$, there will hold

$$\Phi(\Omega^*) \equiv \int_\Omega d\chi_{\Omega^*} - \oint_{\partial\Omega} \beta T \chi_{\Omega^*} ds + 2H \int_\Omega \chi_{\Omega^*} > 0. \tag{A1}$$

Here χ is characteristic function, β denotes cosine of boundary data, T denotes trace operator, and

$$2H = \frac{1}{|\Omega|} \oint_{\partial\Omega} \beta \, ds. \tag{A2}$$

In the case under consideration, we have

$$2H = 2(\beta_1 + \beta_2). \tag{A3}$$

As in the discussion in [10] Chapter 6 and in [16] Sec. 2, we see that there is a Caccioppoli set Ω^0 (perhaps equal to $\emptyset$ or Ω) that minimizes Φ, and Ω^0 is bounded in Ω by a finite number

of non-intersecting circular (extremal) arcs Γ of radius $R = 1/2H$. Further, if any such arc meets $\Sigma = \partial\Omega$ at a point interior to one of the boundary segments, then it does so in an angle γ, measured interior to Ω^0. We suppose that we are faced with this state of affairs, and examine a representative such arc. Since the problem is invariant under the substitutions $u \to -u$, $H \to -H$, $\gamma \to \pi - \gamma$, we may suppose that $\gamma_1 \leq \gamma_2 \leq \pi - \gamma_1$. Since additionally we know that no solution can exist for data in $\mathcal{D}_1^+$, we may limit attention to data in the domain $\mathcal{G}$ indicated in Figure 1A, that is, we may assume also $\gamma_1 + \gamma_2 \geq \pi/2$. We distinguish the various possibilities, in terms of the cosines β_1, β_2 of the angles:

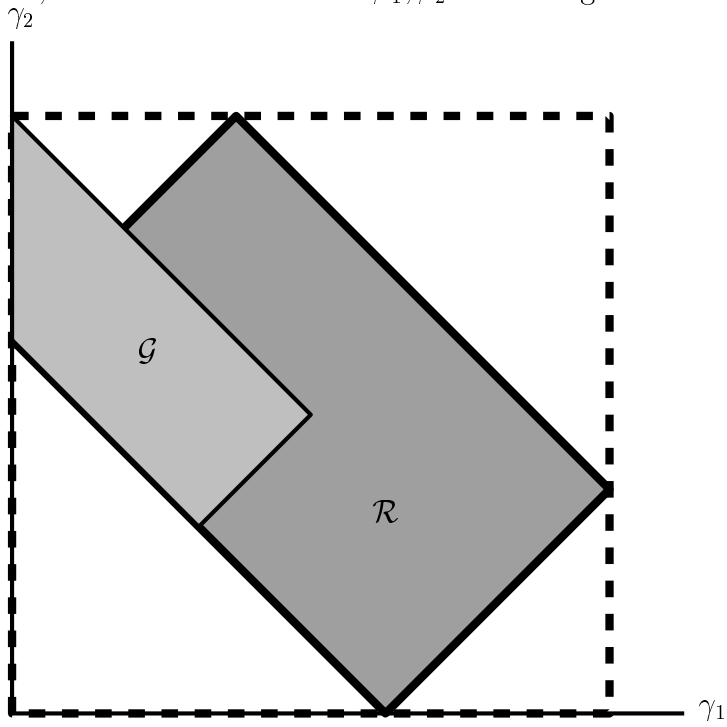

Figure 1A: Data Normalization.

Case 1: $\beta_1 = 0$. Then also $\beta_2 = 0$. The only possible solution is $u \equiv$ const., which does in fact satisfy the conditions of the theorem.

Case 2: $\beta_2 = 0$, $\beta_1 > 0$. Then $2H = 2\beta_1$, and thus the radius of any extremal is $R = 1/2\beta_1$. We consider the various subcases that can occur:

Case 2.1: An extremal Γ cuts two $\beta_2 = 0$ sides in angle $\pi/2$. Then Γ must be linear, contradicting $\beta_1 > 0$.

Case 2.2: An extremal Γ joins the two end points of a $\beta_2 = 0$ side, as in Figure 2A. We assert first that in such a configuration, there holds $\tau \geq \gamma_1$. If $\gamma_1 = 0$, that needs no proof. If $\gamma_1 > 0$ and $\tau < \gamma_1$, one could construct a segment q as indicated in Figure 2A, joining Γ to a $\beta_1 > 0$ side with incident angle γ_1 as in the figure. Replacing the arc l by the segment q, we find that the change in Φ becomes

$$\begin{aligned} \delta\Phi = q - 1 + \beta_1 h &= \frac{l}{\sin\gamma_1}\left\{\sin\tau - \sin\gamma_1 + \sin(\gamma_1 - \tau)\cos\gamma_1\right\} + O(l^2) \\ &\equiv \frac{l}{\sin\gamma_1} f(\tau) + O(l^2). \end{aligned} \tag{A4}$$

We have $f(\gamma_1) = 0$, $f'(\tau) = \cos\tau - \cos(\gamma_1 - \tau)\cos\gamma_1 > 0$, and we conclude $\delta\Phi < 0$ if l is small enough. Thus the configuration cannot minimize, unless $\tau \geq \gamma_1$. If $\tau = \gamma_1 = 0$ then removal of the extremal leads to a change

$$\delta\Phi = -\pi R + \frac{\pi}{2} R < 0 \tag{A5}$$

so that Γ could not minimize. If $\gamma_1 > 0$ then $\tau > 0$, and we can then decrease Φ by replacing a segment of Γ by a segment p orthogonal to the $\beta_2 = 0$ side, as indicated in the figure. We conclude that for the considered case, Γ does not minimize.

Case 2.3: An extremal Γ cuts two $\beta_1 > 0$ sides in angle γ_1. Since $\beta_2 = 0$, Φ is invariant under rigid translation of Γ parallel to these sides, and thus we may assume that Γ passes though two of the vertices, as in Figure 2A, with incident angle γ_1 on the $\beta_1 > 0$ side. This case is thus reduced to the previous one; the configuration cannot minimize.

Case 2.4: An extremal Γ appears as a semicircle, meeting a single $\beta_2 = 0$ side at both end points in angles $\pi/2$, or as a circular arc including a semicircle, meeting a single $\beta_1 > 0$ side in angles γ_1, as indicated in Figure 2A. The former subcase is excluded by (A5); the latter one cannot occur since the radius R of each extremal is $R = 1/2H = 1/2\beta_1 \geq 1/2$.

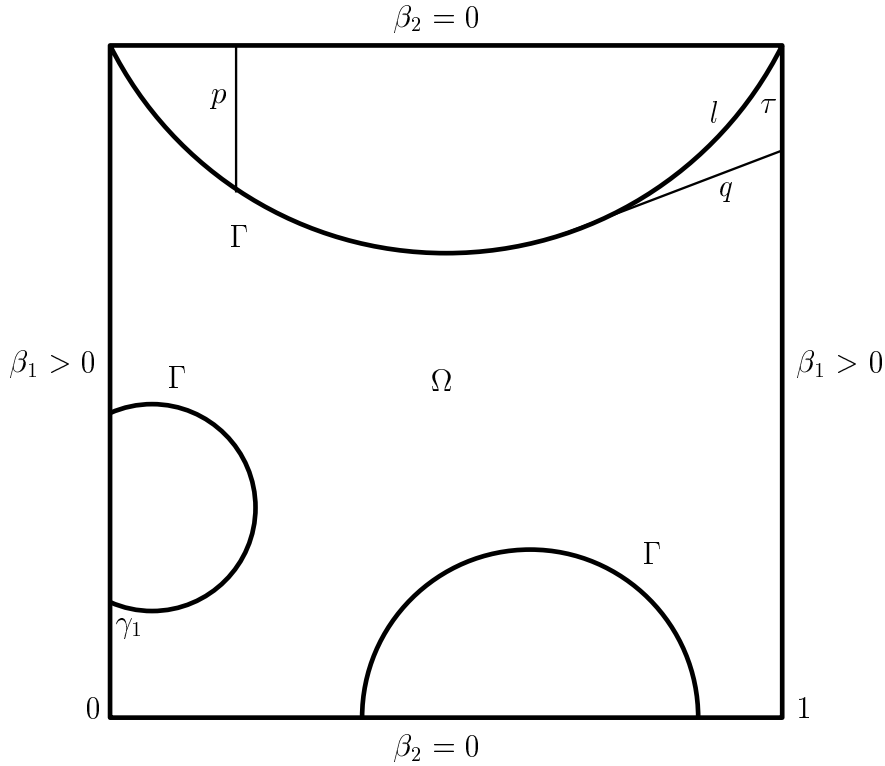

Figure 2A: Extremal configuration; Cases 2.2–2.4.

Case 2.5: An extremal Γ meets a $\beta_2 = 0$ side in angle $\pi/2$, and a $\beta_1 > 0$ side in angle γ_1, as in Figure 3A. We assert that Φ is decreased by removing Γ. In fact, deletion of Γ leads to the change $\delta\Phi = -|\Gamma| + 2\beta_1|\Omega| - h\beta_1$. Fixing attention on the lower extremal in the figure, we have, since the height $y < R$ on Γ, $2\beta_1|\Omega| = 2\beta_1 \int y\,dx < \int dx < \int \sqrt{1+y'^2}dx = |\Gamma|$, and thus $\delta\Phi < 0$. Thus, such a configuration could not minimize.

We may thus assume that neither β_1 nor β_2 vanishes.

Case 3: $\beta_1 + \beta_2 = 0$, $\beta_1\beta_2 \neq 0$. Then $H = 0$ (the minimal surface case) and the extremals are straight lines. No such line can meet interior points of two opposite sides of Ω, as the requirement of equal incident angles would imply $\beta_1\beta_2 = 0$. Nor can such an extremal meet two adjacent sides at interior points, as one would then have $\gamma_1 + \gamma_2 = \pi/2$, while the condition $\beta_1 + \beta_2 = 0$ implies $\gamma_1 + \gamma_2 = \pi$. Suppose Γ passes through a corner point,

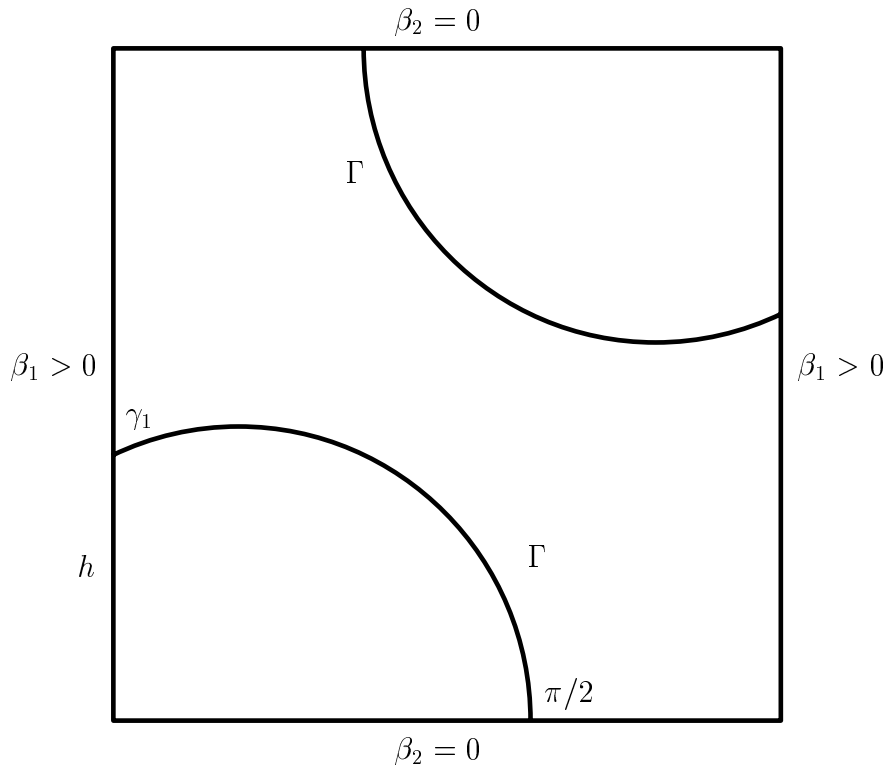

Figure 3A: Extremal configurations; Case 2.5.

as in Figure 4A. Then in the triangle cut off there can be no other extremals, and we find $\Phi = \sqrt{1+h^2} - \beta_1 h - \beta_2 = \sqrt{1+h^2} + \beta_1(1-h) - 1 > 0$, since $\beta_1 > 0$. Since Φ vanishes on the null set, also this case cannot yield a minimizer.

Case 4: $\beta_1 + \beta_2 > 0$, $\beta_1, \beta_2 > 0$. No extremal can meet interior points of adjacent boundary segments, as it would have to do so in the incident angles γ_1, γ_2, as in Figure 5A, and there would then hold $\gamma_1 + \gamma_2 < \pi/2$, whereas we know $\gamma_1 + \gamma_2 \geq \pi/2$ (see Figure 1A). Nor can an extremal from a minimizing set meet a single ($\beta_j > 0$) side, either as indicated or at one or both corner points, as one sees directly that removal of the extremal would decrease Φ. Similarly, no extremal from a minimizing set can begin and end at diagonally opposite points. Were an extremal to meet interior points of two opposite sides as in the figure, we

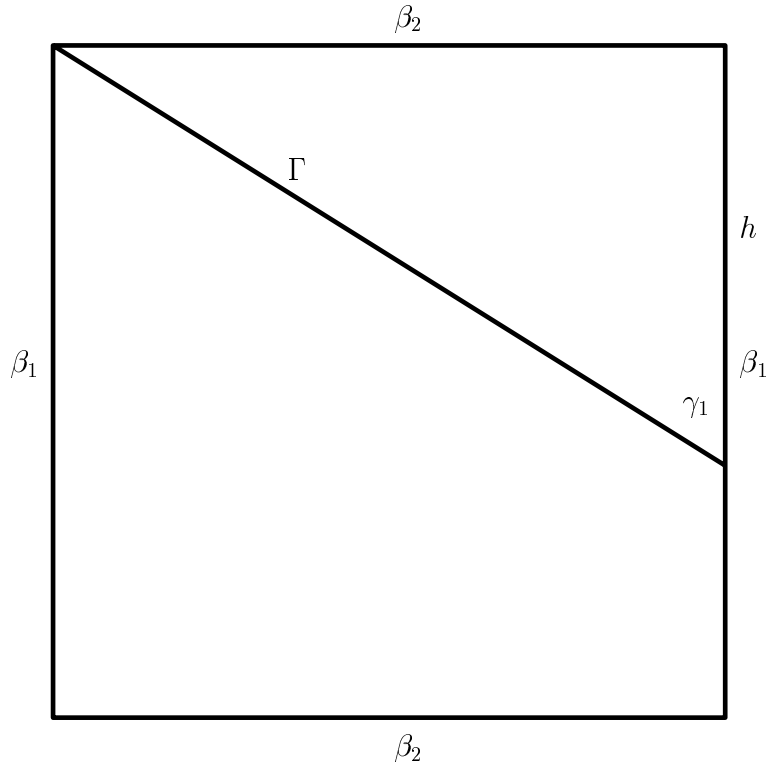

Figure 4A: Extremal in minimal surface case.

would find

$$2R\cos\gamma_j = 1 = \frac{\cos\gamma_j}{\cos\gamma_1 + \cos\gamma_2}\,, \tag{A6}$$

a contradiction. Suppose an extremal passes through a corner point, meeting the adjacent ($\beta_j > 0$) side in angle τ. Then as in Case 2.2 above, $\tau \geq \gamma_j$. Thus again we find the contradiction $\gamma_1 + \gamma_2 < \pi/2$.

Case 5: $\beta_1 + \beta_2 > 0$, $\beta_1 > 0$, $\beta_2 < 0$. Thus, $0 \leq \gamma_1 < \pi/2 < \gamma_2 < \pi - \gamma_1$. As in Case 4, no extremal can meet interior points of opposite sides of the square. Nor can an extremal can have both end points on a single β_1 side, as that would conflict with Theorem 6.11 of [10]. We consider an extremal Γ that meets a β_1 side in angle γ_1 and an adjacent β_2 side in angle

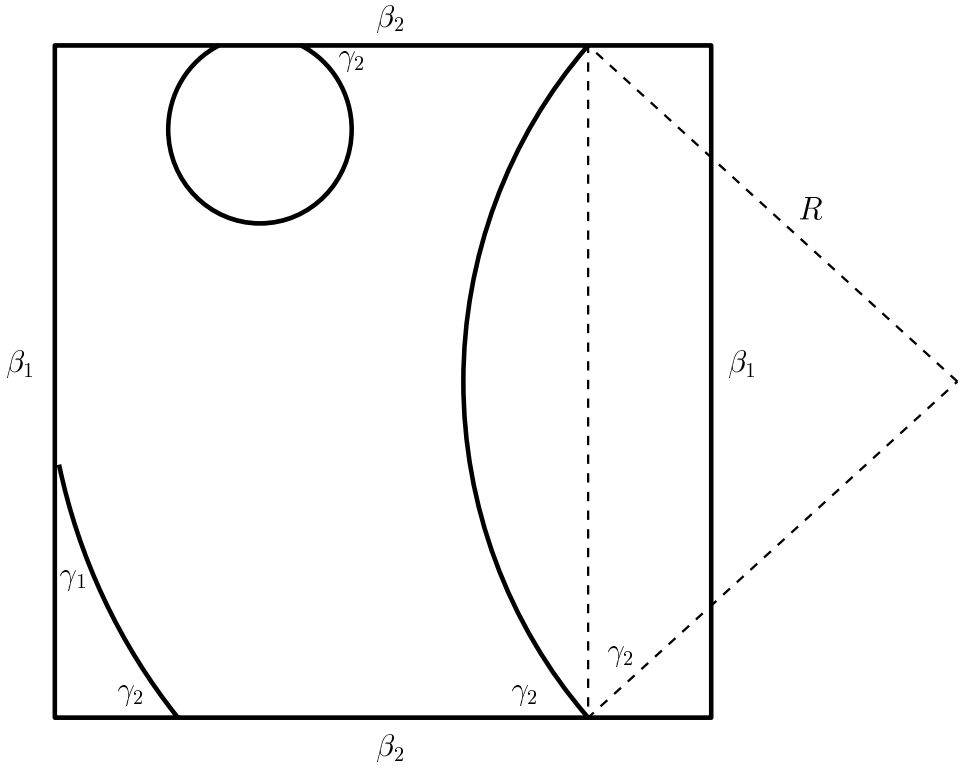

Figure 5A: Extremal configurations; Case 4

γ_2, as in Figure 6A. Removal of such an extremal would result in a change in Φ equal to

$$\begin{aligned}\delta\Phi &= -\int_a^b \sqrt{1+y'^2}dx - (b-a)\beta_2 + \frac{1}{R}\int_a^b \left(y - R\cos(\pi-\gamma_2)\right)dx \\ &= \frac{1}{R}\int_a^b \frac{x^2}{\sqrt{R^2-x^2}}\,dx < 0 \qquad \text{(A7)}\end{aligned}$$

and thus Γ cannot be part of a minimizing set. The same reasoning disposes of the case in which an extremal begins and ends interior to a β_2 side. However, for an extremal joining the two corners of a β_2 side, that procedure no longer works as indicated, and we proceed somewhat differently. Letting τ be the subtended half-angle for such an extremal, as at the top of Figure 6A, we obtain that the change of Φ on removal of the extremal will be

$$\delta\Phi = -\frac{1}{2\sin\tau}\left(\tau + \frac{\sin 2\tau}{2} + 2\beta_2\sin\tau\right) \equiv \frac{1}{2\sin\tau}\,f(\tau), \qquad 0 < \tau \le \frac{\pi}{2}\,. \qquad \text{(A8)}$$

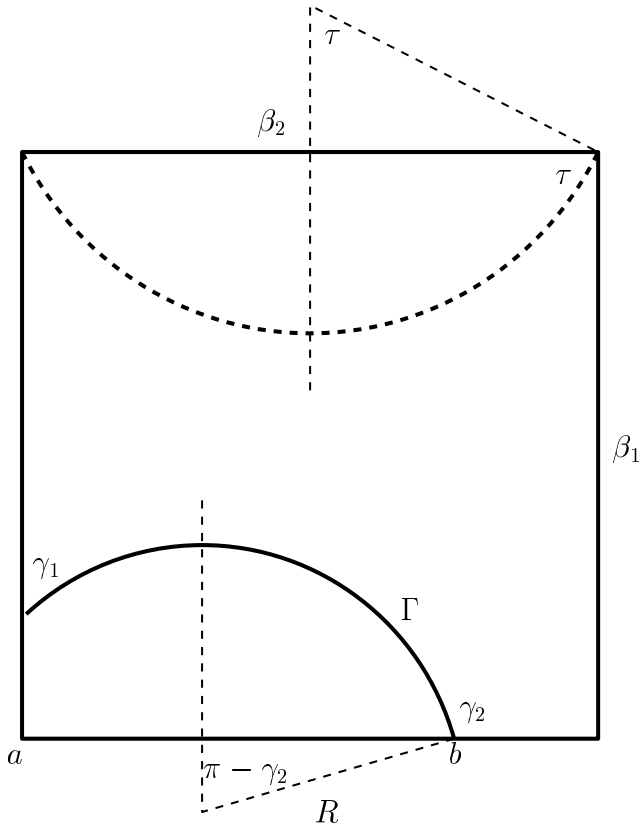

Figure 6A: Extremal configuration; Case 5

We have

$$R = \frac{1}{2\sin\tau} = \frac{1}{2(\beta_1 + \beta_2)} > \frac{1}{2(1+\beta_2)} \tag{A9}$$

so that $\beta_2 > \sin\tau - 1$. Thus $f(\tau) < -\tau - \sin\tau(\cos\tau + 2\sin\tau - 2)$, and $f(0) = 0$, $f(\pi/2) = -\pi/2 < 0$. We calculate $f'(\tau) = (-2\cos\tau + 2 - 4\sin\tau)\cos\tau = g(\tau)\cos\tau$. There holds $g(0) = 0$, $g(\pi/2) < 0$, and $g'(\tau) < 0$ for $\tau < \tan^{-1} 2$, $g'(\tau) > 0$ for larger τ. Thus $g(\tau)$ (and hence also $f'(\tau)$) is negative for all $0 < \tau \leq \pi/2$. We conclude that also $f(\tau) < 0$ in that interval, and hence that the extremal cannot minimize. The remaining cases, of an extremal joining two corners of a β_1 side, and of an extremal joining diagonal corners, can be excluded as in Case 4.

All cases have been covered, and the proof of existence for Theorem 5.1 is complete. Uniqueness up to an additive constant follows from Theorem 3.1 of [15]. (Note that the full strength of this result is needed for uniqueness; Theorem 5.1 of [10] would not suffice, as the solutions are not known to be in the class $W^{1,1}$ in the square.) $\Box$

Corollary 6.3 *For any β in the range $0 \leq \beta \leq 1$, there exists a "Scherck type" minimal surface over a square, achieving "capillary" data $+\beta$ and $-\beta$ on adjacent sides of the square.*

It is this class of surfaces that were studied numerically by Mittelmann and Zhu in [28]. By choosing $\beta = 1$, we obtain the classical Scherk minimal surface $z = \log\cos x - \log\cos y$. The identity of the surface described in the corollary with the Scherk surface follows as above from Theorem 3.1 of [15]. If $\beta < \sqrt{2}/2$ then the surface $u(x, y)$ is continuous and differentiable up to the vertex of the square [21], [5]; if $\sqrt{2}/2 < \beta \leq 1$ then $u(x, y)$ has a discontinuous unit normal at the vertex, and is shown numerically in [28] to be itself discontinuous.

References

[1] M. Athanassenas: *A variational problem for constant mean curvature surfaces with free boundary.* J. reine agnew. Math. **377** (1987) 97–107.

[2] A. Azzam: *Behaviour of solutions of Dirichlet problem for elliptic equations at a corner.* Indian J. Pure Appl. Math. **10** (1979) 1453–1459.

[3] K.L. Brakke: *Surface Evolver.* Susquehanna Univ., Selinsgrove, PA, USA 1996; available from `http://www.geom.umn.edu/software/evolver`.

[4] W.C. Carter: *The forces and behavior of fluids constrained by solids.* Acta Metall. **36** (1988) 2283–2292.

[5] J.-T. Chen, R. Finn, E. Miersemann: *Capillary surfaces in wedge domains: Behavior at the vertex, continuity and discontinuity, asymptotic expansions.* Preprint, Universität Leipzig, 1997.

[6] P. Concus, R. Finn: *On capillary free surfaces in the absence of gravity.* Acta Math. **132** (1974) 177–198.

[7] P. Concus, R. Finn: *Capillary surfaces in a wedge - differing contact angles.* Microgr. Sci. Techn. **VII** (2) (1994) 152–155.

[8] P. Concus, R. Finn: *Capillary Wedges Revisited.* Siam J. Math. Anal. **27** (1996) 56–69.

[9] P. Concus, R. Finn: *Discontinuous behavior of liquids between parallel and tilted plates.* Phys. Fluids **10** (1998) 39–43.

[10] R. Finn: *Equilibrium Capillary Surfaces.* Springer-Verlag 1986.

[11] R. Finn: *Moon surfaces, and boundary behaviour of capillary surfaces for perfect wetting and nonwetting.* Proc. London Math. Soc. **57** (1988) 542–576.

[12] R. Finn: *Local and global existence criteria for capillary surfaces in wedges.* Calc. Var. **4** (1996) 305–322.

[13] R. Finn, J. McCuan: *Vertex theorems for capillary drops on support planes.* Math. Nachr., in press. Available as Math. Sci. Res. Inst. Preprint 1997-077.

[14] R. Finn, T. I. Vogel: *On the volume infimum for liquid bridges.* Z. Anal. Anwendungen **11** (1992) 3–23.

[15] R. Finn, J. Lu: *Regularity properties of H-graphs.* Comm. Math. Helv. **73** (1998) 379–399.

[16] R. Finn, R.W. Neel: *Singular solutions of the capillary equation.* Stanford University Preprint, 1998.

[17] C. Gerhardt: *Global regularity of solutions to the capillarity problem.* Ann. Scuola Norm. Sup. Pisa **3** (1976) 157–175.

[18] C. Gerhardt: *Boundary value problems for surfaces of prescribed mean curvature.* J. Math. Pures Appl. **58** (1979) 75–109.

[19] E. Gonzalez: *Sul problema della goccia appoggiata.* Rend. Sem. Mat. Univ. Padova **55** (1976), 289–302.

[20] F. Joachimsthal: *Demonstrationes theorematum ad superficies curvas spectantium.* J. reine angew. Math. **30** (1846) 347–350.

[21] K. Lancaster, D. Siegel: *Existence and behavior of the radial limits of a bounded capillary surface at a corner.* Pacific J. Math. **176** (1996) 165–194. See also corrections of printer's errors in **179** (1997) 397–402.

[22] D. Langbein: *Stability of liquid bridges between parallel plates.* Microgravity Sci. Techn. **5** (1992) 2–11.

[23] G. Lieberman: *Hölder continuity of the gradient at a corner for the capillary problem and related results.* Pacific J. Math. **133** (1988) 115–135.

[24] J. McCuan: *Symmetry via spherical reflection and spanning drops in a wedge.* Doctoral Dissertation, Stanford Univ., 1995.

[25] J. McCuan: *Symmetry via spherical reflection and spanning drops in a wedge.* Pacific J. Math. **180** (1997) 291–324.

[26] J. McCuan: *Symmetry via spherical reflection.* J. Geometric Analysis. To appear.

[27] E. Miersemann: *On capillary free surfaces without gravity.* Z. Anal. Anwend. **4** (1985) 429–436.

[28] H. D. Mittelmann, A. Zhu: *Capillary surfaces with different contact angles in a corner.* Microgravity Sci. Technol. **IX/1** (1996) 22–27.

[29] W.C. Reynolds, H.M. Satterlee: *Liquid propellant behavior at low and zero g.* In "The Dynamic Behavior of Liquids in Moving Containers," ed. H. N. Abramson, NASA report SP-106 (1966) 387–439.

[30] D. Siegel: *Height estimates for capillary surfaces.* Pacific J. Math. **88** (1980) 471–516.

[31] L. Simon: *Regularity of capillary surfaces over domains with corners.* Pacific J. Math. **88** (1980) 363–377.

[32] D. Strube: *Stability of a spherical and a catenoidal liquid bridge between two parallel plates in the absence of gravity.* Microgravity Sci. Techn. **4** (1991) 104–105.

[33] D. Strube: *Stability of a spherical and a catenoidal liquid bridge between two parallel plates in the absence of gravity.* Correction of a paper by D. Strube. Microgravity Sci. Techn. **5** (1992) 56–57.

[34] N. N. Ural'tseva: *Solution of the capillary problem* (Russian). Vestnik Leningrad Univ. **19** (1973) 54–64.

[35] T. I. Vogel: *Stability of a liquid drop trapped between two parallel planes.* SIAM J. Appl. Math. **47** (1987) 516–525.

[36] T. I. Vogel: *Stability of a liquid drop trapped between two parallel planes.* II. *General contact angles.* SIAM J. Appl. Math. **49** (1989) 1009–1028.

[37] T. I. Vogel: *Numerical results on the stability of a drop trapped between parallel planes.* Report LBL-30486, Lawrence Berkeley Lab., Univ. of Calif., 1991.

[38] T. I. Vogel: *Types of instability for the trapped drop problem with equal contact angles.* In Geometric Analysis and Computer Graphics, P. Concus, R. Finn, D. Hoffman, eds., Math. Sci. Res. Inst. Publ. **17**, Springer-Verlag, New York, 1991, 195–203.

[39] H. C. Wente: *The symmetry of sessile and pendent drops.* Pacific J. Math. **88** (1980) 387–397.

[40] H.C. Wente: *The capillary problem for an infinite trough.* Calc. Var. Partial Differential Equations **3** (1995) 155–192.

[41] H.C. Wente: *Tubular capillary surfaces in a convex body.* In "Advances in Geometric Analysis and Continuum Mechanics," ed. P. Concus and K. Lancaster (1993) 288–298; International Press, 1995.

[42] H.C. Wente: *On the stability of pendant drops.* Bonn Preprint. c. 1985.

[43] L. Zhou: *On the volume infimum for liquid bridges.* Z. Anal. Anwendungen **12** (1993) 629–642.

[44] L. Zhou: *The stability of liquid bridges.* Doctoral Dissertation, Stanford Univ., 1995.

[45] L. Zhou: *On stability of a catenoidal liquid bridge.* Pacific J. Math. **178** (1997) 185–198.

[46] R. Zia, J. Avron, J. Taylor: *The summertop construction: crystals in a corner* J. Statist. Phys. **50** (1988) 727–736.

Lawrence Berkeley Laboratory
and Mathematics Department
University of California
Berkeley, CA 94720 USA
concus@math.berkeley.edu

Mathematics Department
Stanford University
Stanford, CA 94305-2125 USA
finn@gauss.stanford.edu

School of Mathematics
Georgia Institute of Technology
Atlanta, GA 30332-0160 USA
mccuan@math.gatech.edu